

Three-dimensional finite-volume ELLAM implementation

C.I. Heberton & T.F. Russell

University of Colorado at Denver, Denver, Colorado, United States

L.F. Konikow & G.Z. Hornberger

U.S. Geological Survey, Reston, Virginia, United States

ABSTRACT: A three-dimensional finite-volume Eulerian-Lagrangian Localized Adjoint Method (ELLAM) has been developed, tested, and successfully implemented as part of the U.S. Geological Survey (USGS) MODFLOW/MOC3D ground-water modeling package. The USGS ELLAM code simulates solute transport in ground water for a single dissolved constituent subject to advective transport, hydrodynamic dispersion (including mechanical dispersion and diffusion), mixing from fluid sources, and simple chemical reactions (including linear sorption and decay). The implementation conserves mass locally and globally. This ELLAM algorithm incorporates an implicit-in-time, finite-difference approximation for the dispersive and source/sink terms, allowing large transport time increments to be used for greater efficiency. It uses a forward tracking approach to move mass to the new time level, distributing mass among destination cells using approximate characteristic functions. Numerous test cases indicate that the method can usually yield excellent results, even if relatively few transport time steps are used, although the quality of the results is problem dependent.

1 INTRODUCTION

The modular finite-difference ground-water flow model (MODFLOW) developed by the U.S. Geological Survey (USGS) is a widely used and flexible computer program for simulating three-dimensional ground-water systems (McDonald & Harbaugh, 1988, Harbaugh & McDonald, 1996). MOC3D is a solute-transport program that is integrated with MODFLOW and has the capability to calculate changes in concentration of a single solute subject to advection, dispersion, diffusion, fluid sources, decay, and retardation (Konikow et al. 1996, Kipp et al. 1998). MOC3D solves the solute-transport equation in three dimensions using the method of characteristics, with forward particle tracking to represent advection, coupled with either an explicit or implicit finite-difference method to calculate dispersive flux. This approach is optimal for advection-dominated systems, which are typical of many field problems involving ground-water contamination, as it minimizes numerical dispersion. The model assumes that fluid properties are homogeneous and independent of concentration. The solution techniques, however, do not guarantee a mass balance and also require the use of an areally uniform grid.

A Finite-Volume Eulerian-Lagrangian Localized Adjoint Method (FVELLAM) (Healy & Russell, 1993) was developed as an alternative numerical

solution algorithm for the MOC3D transport model. ELLAM (Celia et al. 1990) solves a mass-conservative integral form of the solute-transport equation. The ELLAM algorithm uses an implicit time method for dispersion calculations, which allows for large time steps without stability constraints. ELLAM uses an Eulerian-Lagrangian advection approach, tracking mass through time and then solving a dispersion equation on a fixed-in-space grid. For advection-dominated problems, this has the advantage of generating less numerical dispersion than standard Eulerian approaches using finite-difference and finite-element methods. ELLAM solves integral equations and thus tracks mass associated with fluid volumes, so that it conserves mass locally and globally.

2 GOVERNING EQUATIONS

The ground-water flow, interstitial velocity, and solute-transport equations used in MOC3D are given by Konikow et al. (1996). Solution to the flow equation provides the interstitial velocity field, which couples the solute-transport equation to the ground-water flow equation.

The governing equation for this finite-volume approach is an integral form of the solute-transport equation, which is a statement of conservation of

Report Documentation Page				Form Approved OMB No. 0704-0188	
Public reporting burden for the collection of information is estimated to average 1 hour per response, including the time for reviewing instructions, searching existing data sources, gathering and maintaining the data needed, and completing and reviewing the collection of information. Send comments regarding this burden estimate or any other aspect of this collection of information, including suggestions for reducing this burden, to Washington Headquarters Services, Directorate for Information Operations and Reports, 1215 Jefferson Davis Highway, Suite 1204, Arlington VA 22202-4302. Respondents should be aware that notwithstanding any other provision of law, no person shall be subject to a penalty for failing to comply with a collection of information if it does not display a currently valid OMB control number.					
1. REPORT DATE 2006		2. REPORT TYPE		3. DATES COVERED 00-00-2006 to 00-00-2006	
4. TITLE AND SUBTITLE Three-dimensional finite-volume ELLAM Implementation				5a. CONTRACT NUMBER	
				5b. GRANT NUMBER	
				5c. PROGRAM ELEMENT NUMBER	
6. AUTHOR(S)				5d. PROJECT NUMBER	
				5e. TASK NUMBER	
				5f. WORK UNIT NUMBER	
7. PERFORMING ORGANIZATION NAME(S) AND ADDRESS(ES) California Institute of Technology, Department of Applied Physics, Pasadena, CA, 91125				8. PERFORMING ORGANIZATION REPORT NUMBER	
9. SPONSORING/MONITORING AGENCY NAME(S) AND ADDRESS(ES)				10. SPONSOR/MONITOR'S ACRONYM(S)	
				11. SPONSOR/MONITOR'S REPORT NUMBER(S)	
12. DISTRIBUTION/AVAILABILITY STATEMENT Approved for public release; distribution unlimited					
13. SUPPLEMENTARY NOTES					
14. ABSTRACT					
15. SUBJECT TERMS					
16. SECURITY CLASSIFICATION OF:			17. LIMITATION OF ABSTRACT	18. NUMBER OF PAGES 8	19a. NAME OF RESPONSIBLE PERSON
a. REPORT unclassified	b. ABSTRACT unclassified	c. THIS PAGE unclassified			

mass over the domain of integration. Integration against a “test function” (u) provides the formulation of conservation of mass, including treatment of cell or subdomain boundary conditions and solute decay. The test function effectively specifies the domain of integration for the transport equation by the portion of the space-time domain where its value is nonzero.

If we multiply the solute-transport equation by the test function u and integrate over time and space, we have:

$$\int_{\Omega} \int_0^T \left(u \frac{\partial(\varepsilon C)}{\partial t} + \frac{u}{R_f} \nabla \cdot (\varepsilon \mathbf{C} \mathbf{V} - \varepsilon \mathbf{D} \nabla C) - \frac{u}{R_f} \sum C' W + u \lambda \varepsilon C dt d\mathbf{x} \right) = 0 \quad (1)$$

where Ω is the entire spatial transport subdomain, T is the end of the simulation time period starting at time zero, ε is the effective porosity (dimensionless), C is volumetric concentration (mass of solute per unit volume of fluid, ML^{-3}), t is time (T), R_f is the retardation factor, \mathbf{V} is the interstitial fluid velocity (LT^{-1}), \mathbf{D} is a second-rank tensor of dispersion coefficients (L^2T^{-1}), W is a volumetric fluid sink or source rate per unit volume of aquifer (T^{-1}), C' is the volumetric concentration in the sink/source fluid (ML^{-3}) (if W represents a sink, $C' = C$), and λ is the decay rate (T^{-1}).

The Eulerian-Lagrangian aspects of the method derive from the requirement that the test function satisfy the adjoint equation,

$$\frac{\partial u}{\partial t} + \frac{\mathbf{V}}{R_f} \cdot \nabla u - \lambda u = 0. \quad (2)$$

Thus, for the time step from t^n to t^{n+1} ,

$$u(\mathbf{x}, t) = f(\mathbf{x}, t) e^{-\lambda(t^{n+1}-t)}, \quad (3)$$

where

$$\frac{\partial f}{\partial t} + \frac{\mathbf{V}}{R_f} \cdot \nabla f = 0, \quad (4)$$

so that f is constant along characteristics of the retarded interstitial velocity field. With

$$u = e^{-\lambda(t^{n+1}-t)}, \quad (5)$$

(that is, $f = 1$) we arrive at a statement of global conservation of mass for a time step. For a local conservation equation on each finite-difference cell Ω_l in the transport subdomain, let

$$u_l(\mathbf{x}, t) = f_l(\mathbf{x}, t) e^{-\lambda(t^{n+1}-t)}, \quad (6)$$

where $f_l(x, t^{n+1}) = 1$ on Ω_l and $f_l(x, t^{n+1}) = 0$ elsewhere:

$$\begin{aligned} & \int_{\Omega_l} (\varepsilon C)^{n+1} d\mathbf{x} \\ & + \iint_{\text{supp } u_l \cap \Gamma^{n+1}} \frac{e^{-\lambda(t^{n+1}-t)}}{R_f} (\varepsilon \mathbf{C} \mathbf{V} - \varepsilon \mathbf{D} \nabla C) \cdot \mathbf{n} dt ds \\ & - \int_{t^n}^{t^{n+1}} \int_{\partial \text{supp } u_l} \frac{e^{-\lambda(t^{n+1}-t)}}{R_f} (\varepsilon \mathbf{D} \nabla C) \cdot \mathbf{n} dt ds \\ & - \iint_{\text{supp } u_l \cap \text{supp } W} \frac{e^{-\lambda(t^{n+1}-t)}}{R_f} \sum C' W dt d\mathbf{x} \\ & = e^{-\lambda \Delta t} \int_{\Omega_l^*} (\varepsilon C)^n d\mathbf{x} \end{aligned} \quad (7)$$

where $\partial \cdot$ signifies the spatial boundary of the argument; $\text{supp} \cdot$ denotes the support of a function (that is, the part of its domain where a function assumes a non-zero value); \mathbf{n} is the unit outward normal vector on the specified boundary; Ω_l^* is the part of the spatial domain holding mass at time t^n for destination cell Ω_l at time t^{n+1} under advection; $\Gamma^{n+1} \equiv \partial \Omega \times (t^n, t^{n+1})$ is the space-time boundary at time step $n+1$; and $d\mathbf{x}$ and ds signify differential volume and area, respectively.

Note that equation 7 appears as space-time integrals of the dispersion equations. ELLAM can be viewed as a method of characteristics, tracking mass along streamlines of the flow to accumulate data to the right-hand side of the system of equations.

3 NUMERICAL METHODS

3.1 ELLAM overview

A numerical solution of the three-dimensional ground-water flow equation is obtained by the MODFLOW code using implicit (backward-in-time) finite-difference methods. After the head distribution has been calculated for a given time step or steady-state flow condition, the specific discharge across every face of each finite-difference cell within the transport subdomain is calculated using a finite-difference approximation (see Konikow et al. 1996). The seepage velocity is calculated at points within a finite-difference cell based on linearly interpolated estimates of specific discharge at those points divided by the effective porosity of the cell (see Konikow et al. 1996).

Advection in flowing ground water is simulated by mass tracking along the characteristic curves determined by the seepage velocity. Calculation of advective movement during a flow time step is based on the specific discharges computed at the end of the time step.

As in MOC3D, tracking is performed using linear interpolation of velocity in the direction of the component of interest and piecewise-constant inter-

polation in the other two directions. The approach is to solve a system of three ordinary differential equations to find the characteristic curves $[x = x(t), y = y(t), \text{ and } z = z(t)]$ along which fluid is advected. This is accomplished by introducing a set of moving points that can be traced within the stationary coordinates of a finite-difference grid. Each point corresponds to one characteristic curve, and values of x , y , and z are obtained as functions of t for each characteristic (Gardner et al. 1964). Each point moves through the flow field at a rate governed by the flow velocity acting along its trajectory.

The ELLAM equations suggest that mass is tracked backwards along characteristics to the pre-image of each cell or boundary face. It is not possible, however, to exactly locate all of the mass at the previous time level by backtracking a finite number of points. In order to achieve mass balance, this implementation of the ELLAM algorithm tracks the known mass distribution forward from the old time level to the new time level.

Numerically, this is accomplished by tracking mass forward from the old time level, n , along characteristics. Each cell is divided into subcells, where the number of subcells is determined by parameters NSC, NSR, NSL, specifying the number of subcells in the column, row, and layer direction, respectively. The center of each subcell is the location at time level n of one of the moving points discussed above, which is tracked through the time step under advection. Depending on the exact location of this point in the destination cell at the new time, all of the mass in the subcell may or may not also be found in that destination cell. In order to mitigate the effects of unwarranted mass lumping, subcell mass is distributed among cells neighboring the destination cell using “approximate test functions,” w_l . The value of w_l at the subcell center destination point is the fraction of subcell mass to be distributed to cell l .

This yields the formulation of the time step n term in equation 7,

$$e^{-\lambda \Delta t} \int_{\Omega_l^*} C^n d\mathbf{x} = e^{-\lambda \Delta t} \sum_{j,i,k} \sum_{p=\text{subcell center}} \frac{\Delta x_j \Delta y_i b_{j,i,k}}{(NSC)(NSR)(NSL)} w_l(p^f) C^n(p) \quad (8)$$

where summation runs through all subcells of each cell in the transport subdomain, b is the cell thickness, and p^f is the image of p under forward tracking to the new time level.

The model assumes a source or sink acts uniformly over the entire cell surrounding a source or sink node. For a cell containing a fluid source, a single time step is discretized into a number of sub-time steps determined by parameter NT, and the composite trapezoidal integration rule is applied in time. Mass is tracked to varying locations within the

transport subgrid depending on when in the transport time step the mass enters the system. At each sub-time step, inflow mass is spatially discretized, tracked, and accumulated just like mass that began the time step already in the system, but for the shorter interval.

Sink concentration is assumed to be the average nodal concentration for the transport time step, with the exception of a sink due to evapotranspiration, where sink concentration is taken to be zero. Integration rules are midpoint in space and a one point backward Euler in time.

The quantity mass/porosity in a cell at the new time level t^{n+1} is expressed using the trapezoidal rule for integration, formulated over each cell octant. Concentrations at octant corners are weighted averages of neighboring node concentrations, determined by trilinear interpolation.

Like the algorithms in the previous versions of MOC3D, the ELLAM method approximates total solute flux across the transport subdomain boundary by the advective flux. This approximation is not demanded by ELLAM methods in general, but it is a feature of this particular implementation. This approximation means that boundary-face concentrations are not coupled to cell-center concentrations through the numerical derivative. All mass moving in and out of the transport subdomain can be tracked using the advective algorithm. Mass tracked across outflow boundaries provides data for a system of outflow boundary equations decoupled from the cell equations. User-input inflow concentrations together with the outflow solutions then accumulate on the right-hand side of the system of cell equations.

For an inflow boundary, as for a source, a single time step is discretized into a number of sub-time steps determined by parameter NT. The only difference in the treatment of the inflow boundary from the treatment of the source is that only the two-dimensional boundary face is discretized, while for a source, the entire cell is discretized. For a cell Ω_l , the integration is performed over the intersection of the support of the space-time test function for that cell and the transport subdomain boundary; that is, all mass entering through the boundary and advected to Ω_l during the time step is accumulated to the right-hand side of local equation l .

The right-hand-side outflow boundary integrals are constructed from the mass contributions tracked across the boundary from interior cells, sources, and inflow boundaries during the transport time step. All mass associated with a tracked point that reaches the outflow boundary at any time during the time step is considered to leave the transport subdomain. Test functions are evaluated to distribute mass among neighboring boundary outflow faces.

3.2 Accuracy criteria

An accuracy criterion incorporated in the model constrains the distance that solute mass is advected during each transport time step. A restriction can be placed by the model user on the size of the time step to ensure that the number of grid cells a point moves in the x -, y -, or z -directions does not exceed some maximum. This translates into a limitation on the transport time-step length. If the time step used to solve the flow equation exceeds the time limit, the flow time step will be subdivided into an appropriate number of equal-sized smaller time increments for solving transport.

For advective transport, a mesh density sufficient so that at least four grid nodes are represented across a solute front (or zone of relatively steep concentration gradient) is needed for good accuracy. Similarly, for advecting a peak concentration, the area of the peak should be represented across at least eight nodes of the grid for good accuracy. In such cases, testing suggests that a peak concentration value can be advected with a very small dissipation of the maximum concentration per time step for a variety of Courant numbers. With insufficient mesh density, a peak will dissipate (or decay) rapidly for an initial period of time during which it spreads out and oscillates; thereafter, the numerical decay is very slow and the oscillations do not worsen. A fine discretization of tracked mass (large NSC, NSR, NSL) reduces the rate of peak decay when modeling with many transport time steps. Regardless of the solution accuracy, global mass is conserved.

The accuracy of the dispersion calculation is governed in part by the accuracy of the central-difference approximations to the space derivatives, meaning a finer mesh will result in better accuracy. The implicit formulation for the solution of the dispersion equation is unconditionally stable. This allows for large time steps during the simulation. Because ELLAM solves the dispersion equation along characteristics, thus avoiding large values of the second time derivative of the solution at passage of a steep front, error in calculation of the time derivative may be expected to be small compared to a standard finite-difference solution to an advection-diffusion equation. Some dependence of accuracy of the dispersion calculation on the size of the time step is retained, however. Note that stability does not imply accuracy; accuracy of the solution to the dispersion equation decreases as the time step size increases. On the other hand, modeling with many time steps in order to resolve dispersion to the desired accuracy could result in a loss of peak to numerical dispersion inherent in the treatment of advection, an effect that can be reduced by increasing NSC, NSR, and NSL.

One additional difficulty encountered with implicit temporal differencing results from the use of a

symmetric spatial differencing for the cross-product terms of the dispersion tensor. This creates a potential for overshoot and undershoot in the calculated concentration solution, particularly when the velocity field is oblique to the axes of the grid. A remedy for excessive overshoot and undershoot is to refine the finite-difference mesh. This may, however, increase simulation times.

4 MODEL TESTING AND EVALUATION

The ELLAM simulator was tested and evaluated by running a suite of test cases (see Konikow et al. 1996, Kipp et al. 1998). This suite includes base results generated by analytical solutions and by other numerical models. It spans a range of conditions and problem types so that the user will gain an appreciation for both the strengths and weaknesses of this particular code. All test cases involve steady-state flow conditions.

4.1 One-dimensional flow

The first test case evaluates ELLAM for a relatively simple system involving one-dimensional solute transport in a finite-length aquifer having a third-type source boundary condition. The numerical results are compared to an analytical solution by Wexler (1992, p. 17).

The length of the system is 12 cm; other parameters are summarized in Table 1. The solute-transport equation was solved using ELLAM on a 120-cell subgrid to assure a constant velocity within the transport domain and to allow an accurate match to the boundary conditions of the analytical solution.

Table 1. Parameters used in ELLAM simulation of solute transport in a one-dimensional, steady-state flow system.

Parameter	Value
Transmissivity (T_{xx})	0.01 cm ² /s
ϵ	0.1
Longitudinal dispersivity (α_L)	0.1 cm
Total simulated time	120 s
V_x	0.1 cm/s
$V_y = V_z$	0.0 cm/s
Initial concentration (C_0)	0.0
Source concentration (C')	1.0
Number of rows & layers	1
Number of columns	122
$\Delta x = \Delta y$	0.1 cm
Δz	1.0 cm
NSC	4
NSR=NSL	2
NT	128

Using the explicit finite-difference solution in MOC3D, the dispersion coefficient imposed the limiting stability criteria, and 2401 time increments were required to solve the transport equation. The implicit solver of MOC3D, however, required only 241 moves. ELLAM results for 241 transport time steps, NSC = 4, NSR = NSL = 2, and NT = 128 are essentially identical to the analytical results. Therefore, these solutions are not plotted. Instead, results are plotted for substantially fewer time increments.

A variety of parameter values were evaluated. Figure 1 shows the analytical solution and two ELLAM solutions for a low-dispersion case. For 121 transport time increments, using NSC = 32, NSR = NSL = 2, and NT = 128, there is a very close match between the numerical and analytical solutions. To improve clarity in showing the results for this case, only every fourth data point is shown, except for times less than 10 seconds at $x = 0.05$, where every point is plotted. The efficiency of the numerical solution can be improved by about a factor of four by setting NSC = 4; the results are very similar, so are not plotted, although the concentration is just slightly low at the first grid cell. The simulation took 261 seconds when NSC = 32, but only 60 seconds when NSC = 4. (Simulations were executed on a Data General Unix workstation.) For 12 time increments, using NSC = 4, NSR = NSL = 2, and NT = 128, concentrations at early times and short distances are somewhat low, but elsewhere the results look excellent. Thus, there is an overall good agreement with the analytical results, as well as with the previously published MOC3D results that used 20 times as many time increments. The simulation using 12 time increments took only 15 seconds.

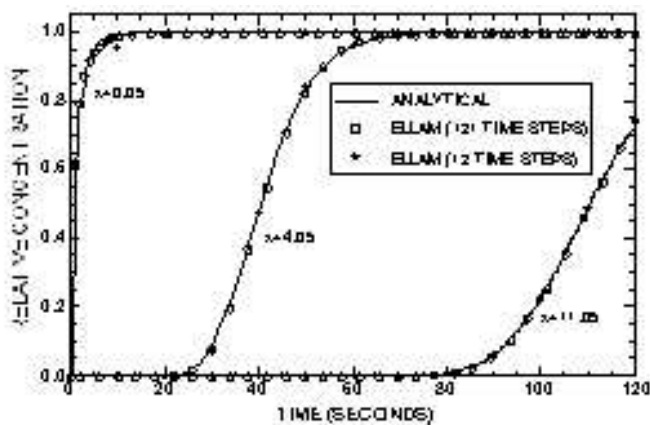


Figure 1. Numerical and analytical solutions at three different locations for solute transport in a one-dimensional, steady flow field.

In all cases described above, the mass-balance error was less than 0.001 percent. In contrast, the mass-balance errors for these problems using the explicit and implicit versions of the method-of-

characteristics code yielded mass-balance errors of up to a few percent in some cases.

4.2 Point initial condition in uniform flow

Three-dimensional solute transport of an instantaneous point source (Dirac initial condition) in a uniform flow field was used as another test problem. An analytical solution for an instantaneous point source in a homogeneous infinite aquifer is given by Wexler (1992, p. 42), who presents the POINT3 code for a related case of a continuous point source. The POINT3 code was modified to solve for the desired case of an instantaneous point source.

The test problem was designed to evaluate the numerical solution for a case in which flow occurs at 45 degrees to the x - and y -axes. This allows us to evaluate the accuracy and sensitivity of the numerical solution to the orientation of the flow relative to the grid. The assumptions and parameters for this test case are summarized in Table 2 and are described in more detail by Konikow et al. (1996).

Table 2. Parameters used in ELLAM simulation of three-dimensional transport from a point source with flow at 45 degrees to x - and y -axes.

Parameter	Value
$T_{xx} = T_{yy}$	10.0 m ² /day
ϵ	0.1
α_L	1.0 m
$\alpha_{TH} = \alpha_{TV}$	0.1 m
Total simulated time	40 days
$V_x = V_y$	1.0275 m/day
V_z	0.0 m/day
Initial concentration at source	1×10^6
Grid location of source	(11,36,4)
Number of rows & columns	72
Number of layers	24
$\Delta x = \Delta y$	3.33 m
Layer thickness (Δz)	10.0 m
$NSC=NSR=NSL$	4
NT	2

The results of the test problem for flow at 45 degrees to the grid are shown in Figure 2. The analytical solution for $t = 130$ days, which provides the basis for the evaluation, is shown in Figure 2a. The ELLAM solution used the analytical solution at $t = 90$ days as the initial conditions, so the elapsed time for the comparison is 40 days. The results using three transport time increments, NSC = NSR = NSL = 4, and NT = 2 are shown in Figure 2b for the horizontal plane of the initial source. ELLAM produces the symmetry characteristic of the analytical solution. There is also slight longitudinal spreading (numerical dispersion).

The numerical results in Figure 2b show some distortion of the shape of the plume relative to the analytical solution. It is not as pronounced, however, as the “hourglass” shape yielded by MOC3D for this problem (see Kipp et al. 1998, Fig. 14). There is a narrowing of the plume calculated with the numerical model, which is characteristic of a grid-orientation effect and is caused primarily by the off-diagonal (cross-product) terms of the dispersion tensor. When flow is oriented parallel to the grid, or when longitudinal and transverse dispersivities are equal, the cross-product terms of the dispersion tensor are zero. Because flow is at 45 degrees to the grid in this test problem, the cross-product dispersive flux terms are of maximum size and negative concentrations are most likely to occur. The calculated concentration field is less accurate in this case largely because the standard differencing scheme for the cross-product dispersive flux terms can cause overshoot and undershoot of concentrations. If the base (or background) is zero concentration, then undershoot will cause negative concentrations. The magnitude of this overshoot and undershoot effect is reduced by using a finer grid.

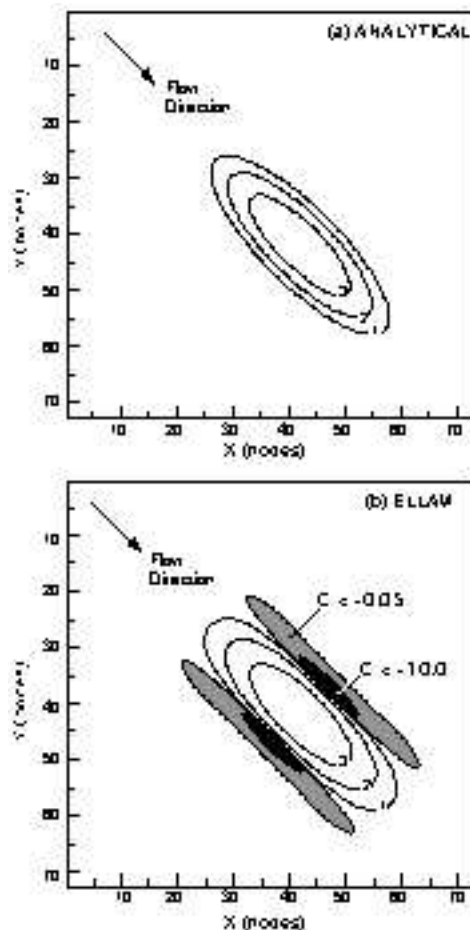


Figure 2. Concentration contours for (a) analytical and (b) ELLAM solutions for transport of a point initial condition in uniform flow at 45 degrees to the x -direction at $t = 130$ days. Contour values are log of concentration.

Indeed, some small areas of negative concentrations were calculated. The extent of the areas of negative concentration are indicated by shading all areas where the relative concentration is less than -0.05 and less than -10.0. Decreasing the size of the transport time increment did not substantially reduce the area over which negative concentrations occurred. The increase in execution time, however, was significant, so the very small improvement does not appear to justify the extra computational costs.

This test case involving a Dirac initial condition with flow at a 45 degree angle to the grid represents a stringent test for any solute-transport model, and the ELLAM results for this case are qualitatively good. Of all the test cases for which ELLAM was evaluated, however, the results were least accurate for this particular set of test conditions.

4.3 Constant source in nonuniform flow

Burnett & Frind (1987) used a numerical model to simulate a hypothetical problem having a constant source of solute over a finite area at the surface of an aquifer having homogeneous properties, but nonuniform boundary conditions, which result in nonuniform flow. Because an analytical solution is not available for such a complex system, we use their results for this test case as a benchmark for comparison with the results of applying the ELLAM algorithm in MOC3D, as was also done by Konikow et al. (1996) and Kipp et al. (1998). Burnett & Frind (1987) used an alternating-direction Galerkin finite-element technique to solve the flow and solute-transport equations in both two and three dimensions. A detailed description of the problem geometry and of the parameters for the numerical simulation are presented by Konikow et al. (1996, p. 55-60).

Cases of both two- and three-dimensional transport were examined for this problem, but only the latter case will be presented here. The grids used in the ELLAM simulations were designed to match as closely as possible the finite-element mesh used by Burnett & Frind (1987). Some differences in discretization, however, could not be avoided because the finite-element method uses a point-centered grid whereas ELLAM uses a block-centered grid. The former allows specifications of values at nodes, which can be placed directly on boundaries of the model domain. Nodes in ELLAM are located at the centers of cells, and block-centered nodes are always one-half of the grid spacing away from the edge of the model domain. Among the small differences arising from the alternative discretization schemes are that, in the ELLAM grid, (1) the modeled location of the 14.25 m long source area is offset by 0.225 m towards the right, and (2) the total length of the domain is 199.5 m.

The input data values for this analysis are listed in Table 3. The top flow layer consisted of constant-head nodes and the solute source.

Table 3. Parameters used for ELLAM simulation of three-dimensional transport from a continuous point source in a nonuniform, steady-state, flow system (described by Burnett & Frind, 1987).

Parameter	Value
K	1.0 m/day
ε	0.35
α_L	3.0 m
α_{TH}	0.10 m
α_{TV}	0.01 m
Total simulation time	12,000 days
Source concentration (C')	1.0
Number of rows	15
Number of columns	141
Number of layers	91
Δx	1.425 m
Δy	1.0 m
Δz	0.2222-0.2333 m
$NSC=NSR=NSL$	4
NT	32

Results for the three-dimensional case based on the test case of Burnett & Frind (1987) are presented in Figure 3, which shows the transport results in a vertical plane at the middle of the plume. The ELLAM plume (Fig. 3b) closely matches that calculated by the finite-element model (Fig. 3a), although the former shows slightly further downstream migration of low concentrations of solute. The ELLAM solution used seven transport time steps whereas the finite-element solution used 40 time steps. The ELLAM solution provides a closer match to the Burnett & Frind (1987) solution than do the previous MOC3D results, which used 381 time steps with the implicit dispersion calculation (Kipp et al. 1998) and 4,218 with the explicit dispersion calculation (Konikow et al. 1996).

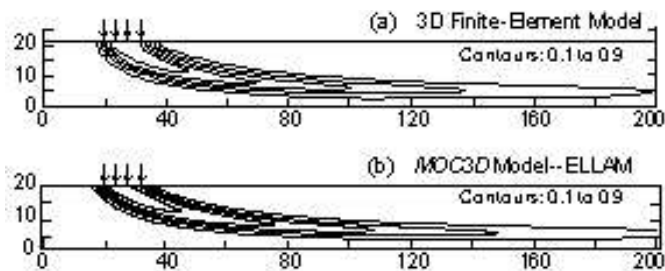


Figure 3. Results of 3-D nonuniform-flow test case: (a) finite-element model using 40 time steps (Burnett & Frind, 1987, Fig. 8c), and (b) ELLAM solution using 7 time steps. Contours are relative concentration (contour interval is 0.2).

4.4 Model availability

The new ELLAM code and a documentation report will be available for downloading over the Internet from a USGS software repository. The repository is accessible on the World Wide Web from the USGS Water-Resources Information Web page at <http://water.usgs.gov/software/> or from an alternative web page for USGS ground-water models at <http://water.usgs.gov/nrp/gwsoftware/>.

5 RELATIVE COMPUTATIONAL AND STORAGE EFFICIENCY

Computer-memory storage requirements for ELLAM are greater than those for the explicit or implicit MOC3D dispersive transport algorithm. The additional arrays required can increase the memory size requirement by as much as a factor of three.

The computational effort required by the ELLAM simulator is strongly dependent on the size of the problem being solved, as determined by the total number of nodes, the NS and NT values, and the total number of time increments. Analyses indicate that the greatest computational effort, as measured by CPU time, is typically expended in the mass tracking routines. For a given problem, computational time may vary significantly as a function of the characteristics of the particular computer on which the simulation is performed, and on which FORTRAN compiler and options were used to generate the executable code.

6 CONCLUSIONS

The accuracy and precision of the numerical results of the implicit ELLAM simulator were tested and evaluated by comparison to analytical and numerical solutions for the same set of test problems as documented previously for MOC3D, although the instantaneous point source problem was modified slightly. These evaluation tests indicate that the solution algorithms in the ELLAM model can successfully and accurately simulate three-dimensional transport and dispersion of a solute in flowing ground water. The numerical methods used to solve the governing equations have broad general capability and flexibility for application to a wide range of hydrogeological problems. To avoid non-physical oscillations and loss of peak concentrations, care must be taken to use a grid having sufficient mesh density to adequately resolve sharp fronts.

Relative to the method of characteristics, the primary advantages of the ELLAM code are that fewer transport time steps need be used and that mass is conserved globally, and relative to other standard

numerical methods, it minimizes numerical dispersion in advection-dominated systems. Using ELLAM with few time steps can provide an accurate and cost-effective way of discerning salient features of the solute-transport process under a complex given set of boundary conditions. Furthermore, the ELLAM algorithm eliminates the previous restriction in MOC3D that the transport grid had to be uniformly spaced.

Acknowledgments

The authors appreciate the helpful model evaluation and review comments provided by USGS colleagues R.W. Healy, K.L. Kipp, D.M. Diodato, and A.M. Shapiro. The research of the second author was supported in part by National Science Foundation Grant No. DMS-9706866 and Army Research Office Grant No. 37119-GS-AAS.

REFERENCES

- Burnett, R.D. & Frind, E.O. 1987. Simulation of contaminant transport in three dimensions, 2. Dimensionality effects. *Water Resources Research* 23(4):695-705.
- Celia, M.A., Russell, T.F., Herrera, I. & Ewing, R.E. 1990. An Eulerian-Lagrangian localized adjoint method for the advection-diffusion equation. *Advances in Water Resources* 13(4):187-206.
- Garder, A.O., Peaceman, D.W., & Pozzi, A.L. 1964. Numerical calculation of multidimensional miscible displacement by the method of characteristics. *Soc. Petroleum Eng. Jour.* 4(1):26-36.
- Harbaugh, A.W. & McDonald, M.G. 1996. User's documentation for MODFLOW-96, an update to the U.S. Geological Survey modular finite-difference ground-water flow model: U.S. Geological Survey Open-File Report 96-485, 56 p.
- Healy, R.W. & Russell, T.F. 1993. A finite-volume Eulerian-Lagrangian localized adjoint method for solution of the advection-dispersion equation. *Water Resources Research* 29(7):2399-2413.
- Kipp, K.L., Konikow, L.F., & Hornberger, G.Z. 1998. An implicit dispersive transport algorithm for the U.S. Geological Survey MOC3D solute-transport model: U.S. Geological Survey Water-Resources Investigations Report 98-4234, 54 p.
- Konikow, L.F., Goode, D.J., & Hornberger, G.Z. 1996. A three-dimensional method-of-characteristics solute-transport model (MOC3D): U.S. Geological Survey Water-Resources Investigations Report 96-4267, 87 p.
- McDonald, M.G. & Harbaugh, A.W. 1988. A modular three-dimensional finite-difference ground-water flow model: U.S. Geological Survey Techniques of Water-Resources Investigations, Book 6, Chapter A1, 586 p.
- Wexler, E.J. 1992. Analytical solutions for one-, two-, and three-dimensional solute transport in ground-water systems with uniform flow: U.S. Geological Survey Techniques of Water-Resources Investigations, Book 3, Chapter B7, 190 p.